2nd URSI AT-RASC, Gran Canaria, 28 May - 1 June 2018

Quantization and Mutual Coupling Effects on Beamforming in Dense Phased Arrays

C.R. Wilke*(1), J. Gilmore (1)
(1) Dept. Electrical and Electronic Engineering, Stellenbosch University, Stellenbosch, South Africa

Abstract

In previous work, the authors investigated the effects of phase quantization on the pointing accuracy and side lobe level of a linear array. These analyses were performed on a *forced excitation* implying direct control over the voltages and currents at the ports of the antennas. By doing it this way, the effects can be directly observed that would otherwise be obscured by mutual coupling. This article is a continuation of this ongoing study in which a practical implementation will be investigated using a *free excitation* model. The coupling parameters are provided by measurements taken from a Dense Dipole Array prototype tile. The pointing accuracy and side lobe level is determined and presented.

1 Introduction

Since around the 1960's, parabolic dishes have traditionally been the instrument of choice for Radio Astronomy. However, today aperture array radio telescopes are being developed internationally for frequencies around 1 GHz [1, 2, 3, 4]. They provide significantly increased fields of view thanks to its multi-beam capabilities which are achieved by means of electronic beam steering in a process called beamforming. As a result, large amounts of data are produced that require processing which will translate to high hardware costs. It is therefore worthwhile to investigate ways in which the hardware complexity can be reduced specifically for the purpose of mass-production and mass-implementation.

In [7] a simple beamforming model was investigated to determine the basic effects of phase quantization on the beamforming performance of a certain array. To isolate the quantization effects, a *forced excitation* model was used implying that the effects of mutual coupling on the radiation pattern of the array is not accounted for. This study serves as a continuation where the beamforming performance metrics are based on a *free excitation* model. The required mutual coupling parameters are based on measurements taken from a Dense Dipole Array prototype tile.

2 Quantized Beamforming: Free Excitation Analyses

The array factor of an ideal planar array (AF_{I}) is given as:

$$AF_{\mathrm{I}} = \sum_{n=0}^{N-1}\sum_{m=0}^{M-1} A_{\mathrm{mn}} e^{\psi-\beta}, \tag{1}$$

where ψ is defined as:

$$\psi = kd\left(m\sin\theta\cos\phi + n\sin\theta\sin\phi\right), \tag{2}$$

and β, the phase delay (or phase shift) set at each element by the beamformer to steer the array towards (θ_0, ϕ_0), is defined as:

$$\beta = kd\left(m\sin\theta_0\cos\phi_0 + n\sin\theta_0\sin\phi_0\right). \tag{3}$$

In a practical beamformer β is limited to a finite set of values which are integer multiples of the phase resolution β_{res} determined according to the number of bits as:

$$\beta_{\mathrm{res}} = \frac{2\pi}{2^B}. \tag{4}$$

The phase term, β, is now redefined as a quantized phase (β_{q}) and is calculated as:

$$\beta_{\mathrm{q}} = \left\{\frac{\beta}{\beta_{\mathrm{res}}}\right\}\beta_{\mathrm{res}}, \tag{5}$$

where the curled braces indicates a rounding operator in which the fraction is rounded to the nearest integer. In this way, β_{q} is selected to be the value closest to β at element (m,n).

The quantized array factor (AF_{Q}) can now be expressed as:

$$AF_{\mathrm{Q}} = \sum_{n=0}^{N-1}\sum_{m=0}^{M-1} A_{\mathrm{mn}} e^{\psi-\beta_{\mathrm{q}}}. \tag{6}$$

By using a free excitation model, the total radiation pattern $(F(\theta,\phi))$ of a phase quantized planar array including mutual coupling effects can be calculated with an *active-element pattern* [5, 6] approach which is mathematically

defined as the sum of the product of the array factor (Equation 6) and the active element pattern $f_{\mathrm{mn}}(\theta,\phi)$:

$$F(\theta,\phi) = \sum_{n=0}^{N-1}\sum_{m=0}^{M-1} A_{\mathrm{mn}} e^{\psi-\beta_{\mathrm{q}}} f_{\mathrm{mn}}(\theta,\phi). \quad (7)$$

If it is known that the active element pattern of a central element in the array is a good representation of the average pattern of all the embedded element patterns in the array then it can be used on its own to determine $F(\theta,\phi)$ as:

$$F(\theta,\phi) = AF_{\mathrm{Q}} f(\theta,\phi). \quad (8)$$

3 Dense Dipole Array Measurements

S-Parameter measurements taken from a 10×10 Dense Dipole Array (DDA) prototype tile (shown in Figure 1) revealed that the radiation pattern of a central active element is a good average representation of the radiation pattern of the full tile. This was observed by comparing the coupling between a central element and its nearest neighbour and the coupling between a central element and an edge element. This is shown in 2.

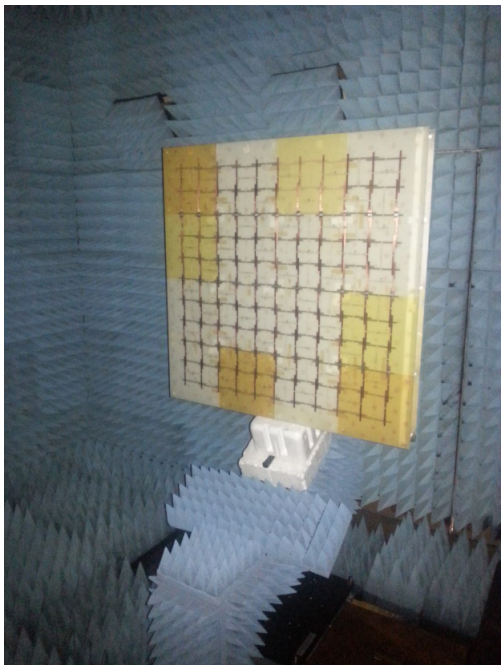

Figure 1. DDA prototype tile mounted in the anechoic chamber at Stellenbosch University

With this observation in mind, it is possible to conduct simulations on a larger theoretical array, which for the purposes of this study is chosen to be the size of 4 DDA tiles stacked together to form a 20×20 array.

Measurement of the active element pattern was limited to the E- and H-planes due to the physical size of the prototype tile and the available measurement equipment. The

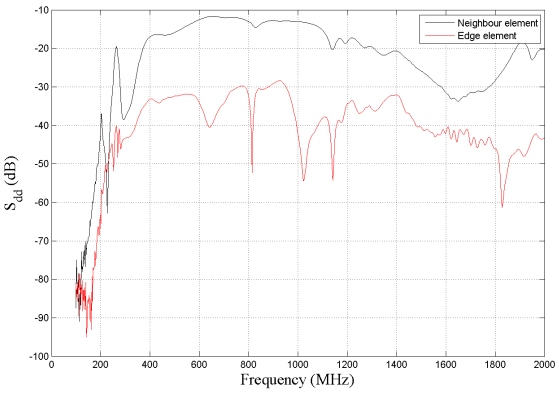

Figure 2. Comparison of the coupling between a central element to a close neighbour and to an edge element

respective patterns are shown at three different frequency points in Figures 3 and 4.

Based on Equation 8, simulations are performed to determine the side lobe level and pointing accuracy under the influence of phase quantization. The value of $f(\theta,\phi)$ is substituted by the measured gain patterns, however, now reduced to the $\phi = 0°$ and $\phi = 90°$ planes, which also corresponds to the principal planes of the array.

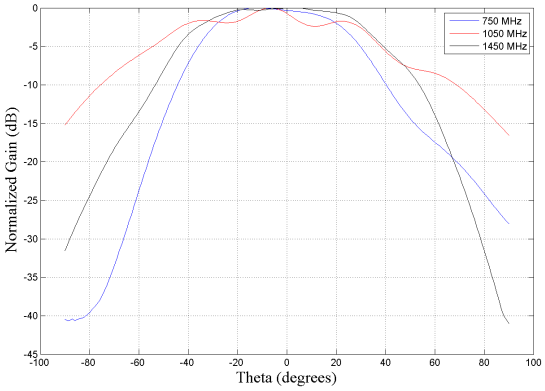

Figure 3. Normalized co-polar E-plane gain pattern

4 Results

The mean scan error for both planes are shown in Figures 5 and 6 for one, two and three-bit phase quantization. Also note that the results are determined as a function of a density ratio (R) defined as:

$$R = \frac{d_0}{d}, \quad (9)$$

where d is the physical inter-element spacing of the DDA (90 mm), and d_0 is a reference inter-element spacing which for the purposes of studying dense arrays, is set to $\lambda/2$. By

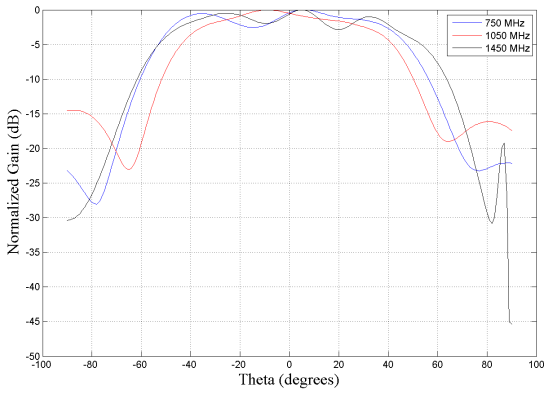

Figure 4. Normalized co-polar H-plane gain pattern

doing it this way, the results are determined as a function of the electrical length between the elements which is a particularly relevant parameter in wide-band arrays.

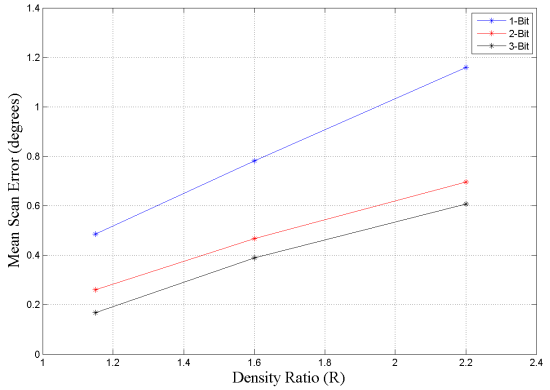

Figure 5. Mean scan error as a function of R and B in the E-plane

The gain patterns are not uniform and it is expected that this will have an impact on the scan accuracy. Additionally, it is expected that the half-power edges of the active patterns will have the largest impact on the scan accuracy. This is because the main beam experiences a significant deformation at these points effectively shifting the maximum point. It is also expected that this observation will increase as the array factor beamwidth increases, and therefore an increase in mean error is observed with an increase in R, for all B values.

However, with these effects in mind it is still significant to notice that the mean scan error is mostly below 1°. The reason for this significance can be attributed to the fact that the simulation array model is relatively small in a practical sense and it is expected that the scan accuracy will improve significantly as a function of increasing aperture.

Furthermore, it is also seen that the phase resolution has a dominant contribution to the scan accuracy, which is significant because direct control is available over the phase res-

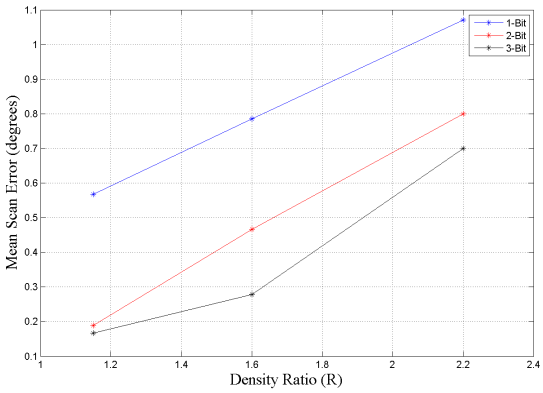

Figure 6. Mean scan error as a function of R and B in the H-plane

olution of the beamformer while the active element pattern is much harder to optimize for an improved scan accuracy.

The side lobe level is analysed using the following signal to quantization noise ratio (SQNR) expression:

$$\mathrm{SQNR} = \frac{|AF_{\mathrm{I}}(\theta_0,\phi_0)|^2}{\mathrm{E}\left[|F(\theta,\phi) - AF_{\mathrm{I}}(\theta,\phi)|^2\right]}, \tag{10}$$

Where the denominator is described as the mean value of the average pattern noise power for all possible scan directions in the visible region. The numerator is the power in the intended scan direction of the ideal power pattern, which in this case is simply the array factor.

The SQNR results for both the E- and H-planes are shown in Figures 7 and 8 respectively.

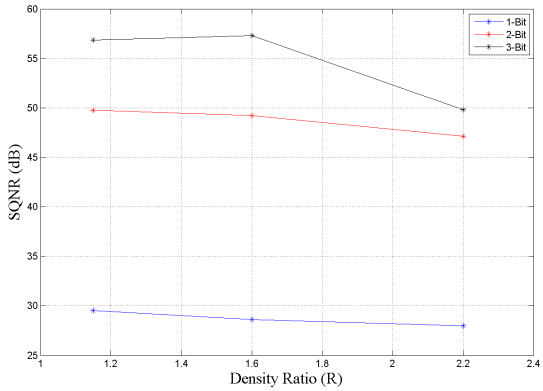

Figure 7. SQNR as a function of R and B in the E-plane

As expected, the SQNR increases as the phase resolution increases. This can be described by the observations made by the author in [7] where it was seen that the quantization lobe amplitude, which is the dominant source of power pattern noise, reduces strongly as a function of increasing

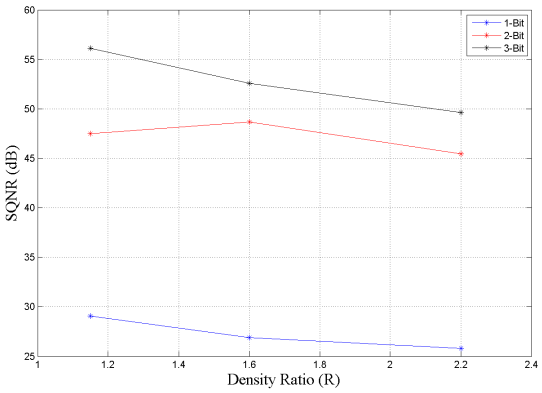

Figure 8. SQNR as a function of R and B in the H-plane

phase resolution. The average SQNR level in both planes are similar, however, a difference in behaviour (or trend) is noticed. This can directly be attributed to the variations in the embedded element patterns. For some scan angles the main beam will be attenuated relative to the side lobe level, which results in a higher average pattern noise. This can further be confirmed by comparing the results of both planes.

5 Conclusion and Future Work

The pointing accuracy and side lobe level of a quantized beamforming model was investigated. It served as a continuation on a previous study by extending the original model to a planar array with mutual coupling.

It was shown that the average pointing accuracy is mostly below one degree for the full scan range in the visible region. It is expected that a further decrease will be observed with an increase the array size. The exact extent of this will be investigated in future work.

The side lobe level trends were established using the SQNR. It was observed that the decrease in quantization lobe amplitude level as a function of phase resolution had a significant impact on the SQNR. Furthermore it was observed that the active element pattern has a significant contribution to the SQNR when comparing the results of both planes.

It should be mentioned that this work additionally serves as a first ever study into the beamforming capabilities of the DDA. The DDA forms part of the candidate technology group of the Mid-Frequency Aperture Array of the Square Kilometre Array which renders these results particularly relevant.

In future work the same effects will be investigated, but with the extension of using different beamforming algorithms and larger simulation models for increased practicality.

References

[1] G. W. Kant, P. D. Patel, S. J. Wijnholds, M. Ruiter, and E. van der Wal, "EMBRACE: A Multi-Beam 20,000-Element Radio Astronomical Phased Array Antenna Demonstrator," *IEEE Transactions on Antennas and Propagation*, vol. 59, no. 6, pp. 1990–2003, jun 2011. [Online]. Available: http://ieeexplore.ieee.org/document/5722987/

[2] J. G. Bij de Vaate, S. A. Torchinsky, A. J. Faulkner, Y. Zhang, A. Gunst, P. Benthem, I. M. van Bemmel, and G. Kenfack, "SKA Mid Frequency Aperture arrays: Technology for the ultimate survey machine," in *2014 XXXIth URSI General Assembly and Scientific Symposium (URSI GASS)*. IEEE, aug 2014, pp. 1–4. [Online]. Available: http://ieeexplore.ieee.org/document/6929991/

[3] J. G. B. de Vaate and A. J. Faulkner, "Aperture arrays for the Square Kilometre Array," in *2012 International Conference on Electromagnetics in Advanced Applications*. IEEE, sep 2012, pp. 618–621. [Online]. Available: http://ieeexplore.ieee.org/document/6328700/

[4] J. Gilmore, "Design of a Dual-Polarized Dense Dipole Array for the SKA Mid-Frequency Aperture Array by," Ph.D. dissertation, 2016.

[5] W. L. Stutzman and G. A. Thiele, *Antenna Theory and Design*, second edi ed. John Wiley & Sons, Inc.

[6] C. Balanis, *Antenna Theory and Design*, 1982, vol. 28, no. 3. [Online]. Available: http://digital-library.theiet.org/content/journals/10.1049/ep.1982.0113

[7] C. R. Wilke, J. Gilmore, and D. B. Davidson, "Reducing the maximum quantization scan error in dense phased arrays," in *2017 International Conference on Electromagnetics in Advanced Applications (ICEAA)*. IEEE, sep 2017, pp. 1268–1271. [Online]. Available: http://ieeexplore.ieee.org/document/8065503/